A Rare Earth Metal Catalyzed Aerobic Dehydrogenation of *N*-Heterocycles

Ting Zhang, Yongheng Lv,Zhenguo Zhang, Zhenhua Jia,* and Teck-Peng Loh*

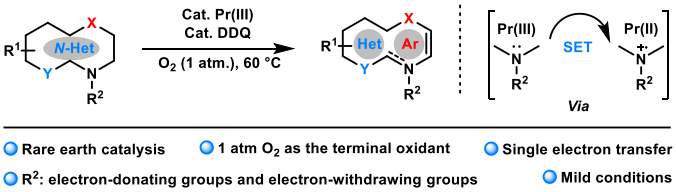

ABSTRACT: Rare earth metals exhibit high catalytic activity and selectivity in various organic reactions due to their unique electronic properties. Among them, praseodymium has been shown high catalytic activity under mild reaction conditions compared with transitional metals. Here, we report a strategy of Pr-catalyzed aerobic dehydrogenative aromatization of saturated *N*-heterocycles to produce 7 classes of products with abroad substrate scope. Preliminary mechanistic studies indicated the oxidation state of Pr probably changed during the reaction from +3 to +2 *via* a single electron transfer process.

Rare earth metals are widely utilized in various applications such as materials, batteries, electronics, and medical imaging reagents, among others, owing to their exceptional chemical, optical, and electronic properties.[1-5] In the domain of organic synthesis, rare earth metals are often employed as Lewis acids to expedite desired organic transformations with remarkable efficiency, selectivity, and stability[6]. One of the distinctive aspects of rare earth metals in catalysis is their ability to form diverse oxidation states, wherein the most stable oxidation state is typically +3. This characteristic enables them to effectively activate and stabilize intermediates during the catalytic process, further enhancing their catalytic prowess. The large electron reservoir of lanthanide metals,the Lewis acidic character of the Ln^{3+} ions and their intermediate electronegativity compared to lithium or magnesium can provide unique reactivity patterns.[6]

For example, Praseodymium, an important rare earth metal, has found diverse applications as a crucial component in high-performance magnets, glass, ceramics, alloys, and more. However, despite its versatility, praseodymium and its complexes have been scarcely utilized in organic synthesis. There are only a few instances where praseodymium organometallic complexes were prepared and employed for carbon-carbon bond formation.[7] Imamoto *et al.* discovered that a simple praseodymium chloride salt combined with lithium reagents could efficiently yield alcohols from carbonyl compounds under mild conditions.[8] Priefer *et al.* reported that the *in-situ* formed reagents of Pr^0/TMSCl induced carbon-carbon coupling of ketones to generate pinacols.[9] Zhang *et al.* studied the Barbier-type reaction with praseodymium reagents, which showed efficient insertion of the carbon-iodide bond of allyl iodide to yield the organometallic complex, reacting with ketones under mild conditions without any additives.[10] In 2017, Pan *et al.* discovered that $Pr(OTf)_3$-catalyzed regioselective amination using azides could produce C3-N-substituted coumarins.[11] Nitrogen heterocycles are abundant in natural products and pharmaceuticals, dehydrogenation of partially saturated aromatic N-heterocycles shows utmost importance for the synthesis of heterocycles.[12]

Scheme1. The Application of Praseodymium in Organic Synthesis

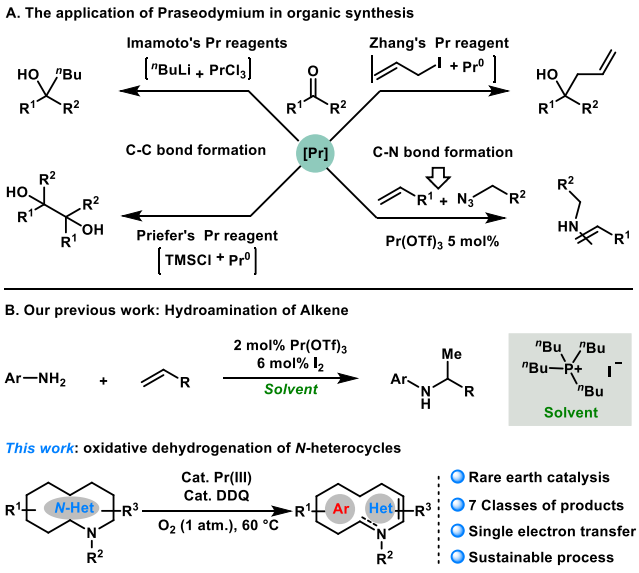

Our group previously reported an efficient $Pr(OTf)_3$-catalyzed intermolecular hydroamination of unactivated alkenes with anilines in an ionic solvent to obtain the Markovnikov products.[13] In continuation of our efforts towards green synthesis,[13] we hereby report an efficient protocol of Pr-catalyzed aerobic dehydrogenative aromatization of saturated *N*-heterocycles. The reaction is also tolerant with electron-withdrawing groups

substituted at the N-1 position and this process probably involved a single electron transfer process (Scheme 1).

Table 1.Optimization of Reaction conditions[a]

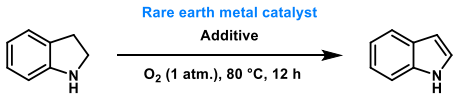

1 2

entry	Rare earth catalyst (mol%)	Additive	Yield of **2** (%)
1	$PrCl_3·7H_2O$ (10 mol%)	NA	67
2	$Pr(NO_3)_3·6H_2O$ (10 mol%)	NA	21
3	$Pr(SO_4)_3·8H_2O$ (10 mol%)	NA	37
4	$Pr(OAc)_3·H_2O$ (10 mol%)	NA	n.d.
5	$Pr(OTf)_3$	NA	26
6	$CeCl_3·7H_2O$ (10 mol%)	NA	58
7	$EuCl_3·6H_2O$ (10 mol%)	NA	57
8	$SmCl_3·6H_2O$ (10 mol%)	NA	59
9	$NdCl_3·6H_2O$ (10 mol%)	NA	60
10	$PrCl_3·7H_2O$ (10 mol%)	NA	63[b]
11	$PrCl_3·7H_2O$ (10 mol%)	DDQ (15 mol %)	98[c]
12	$PrCl_3·7H_2O$ (10 molt%)	DDQ (10 mol %)	98[c]
13	$PrCl_3·7H_2O$ (10 mol%)	DDQ (7.5mol %)	93[c]
14	$PrCl_3·7H_2O$ (7.5 mol%)	DDQ (15 mol %)	98[c] (90)[d]
15	$PrCl_3·7H_2O$ (5 mol%)	DDQ (7.5mol %)	88[c]

[a]Reaction conditions: **1** (0.2 mmol), Rare earth metalSalt (10 mol%), in 1,4-Dioxane (1.0 mL) at 80 °C under 1 atm O_2 for 12h. Yield is based on **1** and was determined by ^{1}H-NMR analysis by using CH_3NO_2 as an internal standard. [b]In THF. [c]At 60°C. [d]Isolated yields.

Aerobic dehydrogenative aromatization has recently emerged as a powerful tool for synthesizing diverse *N*-heterocycles.[14-22] To optimize the reaction conditions, we began our study with indoline as the model substrate, using rare earth metal salts as the catalysts (Table 1, entries 1-10). In the absence of additives, indole was obtained in 67% yield with 10 mol% of $PrCl_3·7H_2O$ as the catalyst at 80 °C (Table 1, entry 1). We systematically screened other parameters of the reaction conditions, and promising results were demonstrated using solvents such as 1,4-dioxane and THF, yielding indole in 67% and 63% yields, respectively (Table 1, entries 1 and 10). We also screened different additives and ligands (Tables S6-S7), and to our delight, adding 15 mol% DDQ as the co-oxidant increased the reaction yield to 98% at a lower temperature of 60 °C (Table 1, entry 11). The amounts of $PrCl_3·7H_2O$ and DDQ were adjusted slightly, and the results were shown (Table 1, entries 11-15). Finally, using 7.5 mol% of $PrCl_3·7H_2O$ as the catalyst, 15 mol% DDQ as the co-oxidant, 1,4-dioxane as the solvent, and under O_2 atmosphere, indole was isolated in 90% yield at 60 °C in 12 hours (Table 1, entry 14).

Next, we examined diverse classes of N-heterocycles under the optimal reaction conditions(Scheme 2). We first explored a broad range of indolines and successfully obtained the corresponding indole products in good to excellent yields (**2a-2ab**). Even N-methyl indoline was suitable, producing N-methyl indole in 93% yield (**2b**). When we tested other substituted groups at the N1 position of indolines, we found that benzyl and phenyl groups were well-tolerated, delivering the desired products (**2c**) and (**2d**) in 70% and 85% yields, respectively. Although electron-withdrawing groups such as acetyl, tert-butoxycarbonyl, and *p*-toluenesulfonyl groups resulted in lower yields (**2e-2h**), they were still tolerated in our protocol, with the synthetic intermediate (**2g**) of Enzastaurin generated in 78% yield to demonstrate the potential application of our aerobic dehydrogenative aromatization strategy. We also screened other substituents at the C2 and C3 positions of indolines. A methyl group at the C2 position, for instance, yielded the corresponding product in 79% yield (**2i**), while an aromatic group, phenyl-substituted at the C2 position, resulted in a lower yield of 58% (**2j**). Electron-withdrawing groups, such as an ester group at the C2 position, were successfully introduced in a 97% yield (**2k**), while a 70% yield of the target product at the C3 position was isolated (**2l**). Halogen groups at the benzyl ring of indolines were also subjected to the current protocol, and the corresponding products were obtained in 76-92% yields, paving the way for further transformations (**2m-2r**). A methyl substituent at the C5 position was well-tolerated, yielding **2s** in 93% yield, while a methoxyl substitute had a negative impact, producing **2t** in 50% yield. Other functional groups at the C5 position, including cyano, formyl, ester, hydroxyl, and amine, were applicable in this reaction. To our surprise, a nitro-substituted indoline at the C6 position exhibited efficient tolerance, yielding the desired product in 98% yield (**2x**). Moreover, with *N*-hetero indoline as the substrate, the corresponding *N*-hetero indole was obtained in 40% yield (**2ab**). It is noteworthy that the decarboxylation process occurred, yielding **2a** in 40% yield when the carboxyl group occupied the C2 position of indoline. To showcase the general application of our protocol, other *N*-heterocycles such as nifedipine (**3**), quinoline (**4**), benzoxazole (**5**), quinazoline (**6**), quinazolone (**7**), and β-carboline (**8**) were obtained in 30-86% yields from their saturated precursors under the standard conditions (**5-8**).

Scheme 2.Scope of substrate[a]

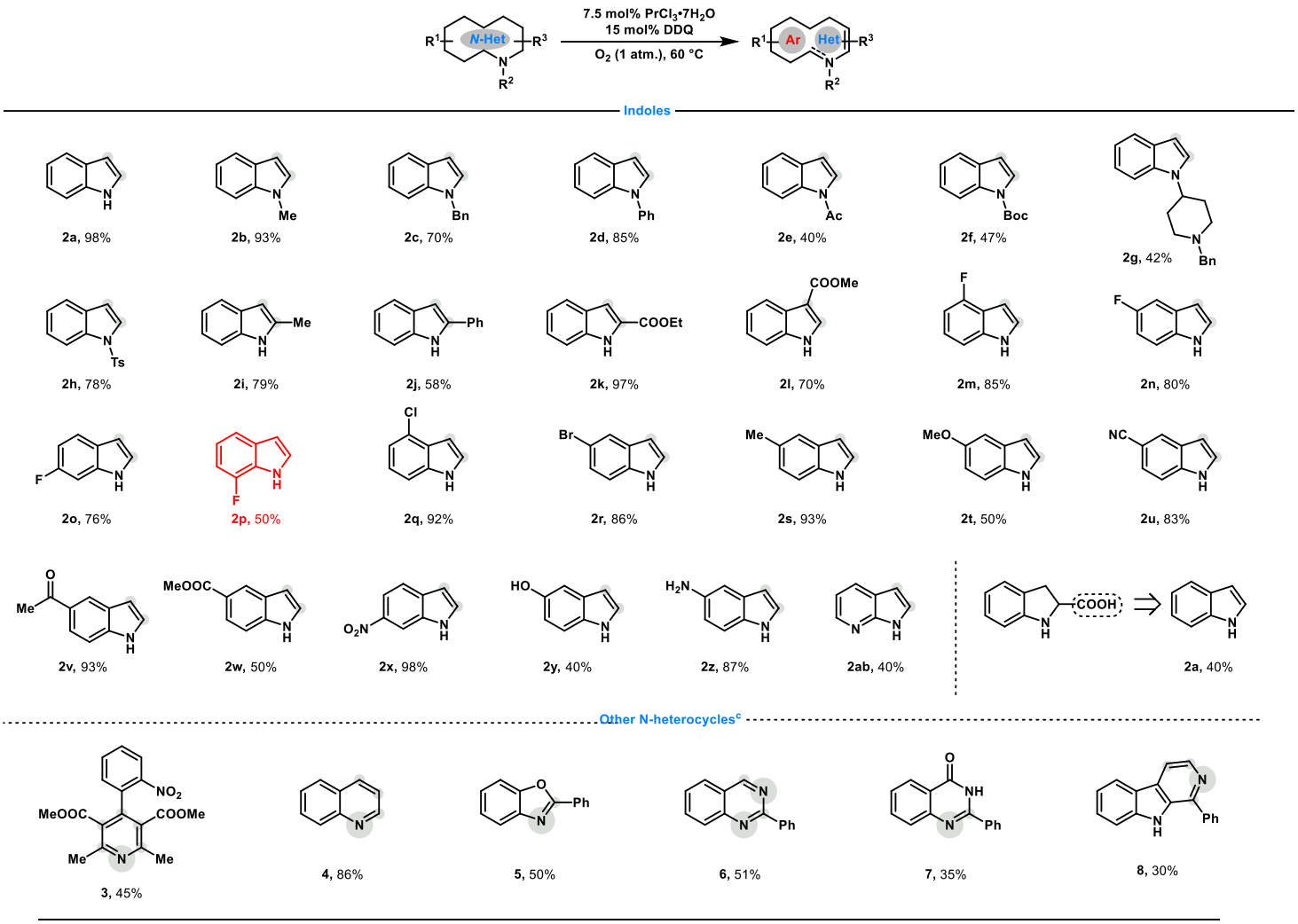

[a]Reaction conditions: **1** (0.2mmol), $PrCl_3 \cdot 7H_2O$ (0.015 mmol), DDQ (0.03mmol) in 1,4-Dioxane (1.0 mL) at 60 [o]Cunder 1 atm O_2 for 12 h.[b]Yields of isolated products are given.[c]At 110 [o]C.

As shown in (Scheme 3-1), we also demonstrated the potential utility of this reaction to synthesize **2** on a gram scale. To elucidate the probable mechanism for this rare earth metal catalyzed aerobic dehydrogenative aromatization reaction, we first performed a series of control experiments (Scheme 3-2). In the absence of $PrCl_3 \cdot 7H_2O$, the efficiency of the model reaction decreased significantly, resulting in only 35% yield of **2**. It is noteworthy that **2** was generated in 65% yield when the reaction was conducted in air, but only 7% of the target product was detected in an argon atmosphere, indicating that oxygen molecules were necessary for the efficient transformation. A kinetic isotope effect (KIE) experiment was also carried out independently by intramolecular competition. Deuterated N-methylindolines (***S*2q-*d*$_2$**)were synthesized according to literature procedures,,The kinetic isotope effect (KIE) experiments was conducted to achieve the rates of dehydrogenation with **2q-*d*$_2$**. An obvious deuterium KIE was observed as 2.23, as proved by the isolation of **2q-*d*$_2$** in 31% yield (Scheme 3-3).

To investigate the possible pathway, we also compared the UV-visible absorption spectra(Figure1). From the spectra shown in Figure 1, which include indoline (orange), DDQ (green), $PrCl_3 \cdot 7H_2O$ (purple), and indicated samples of different combinations, we found that the major absorption of $PrCl_3 \cdot 7H_2O$ and indoline distributed beyond 250 nm and around 300 nm, respectively. In addition, there was an obvious absorption peak at 350 nm in the mixture curve of praseodymium and indoline, revealing the direct coordination between the rare earth metal and the substrate.

Scheme 3. Gram scale synthesis and preliminary mechanistic study

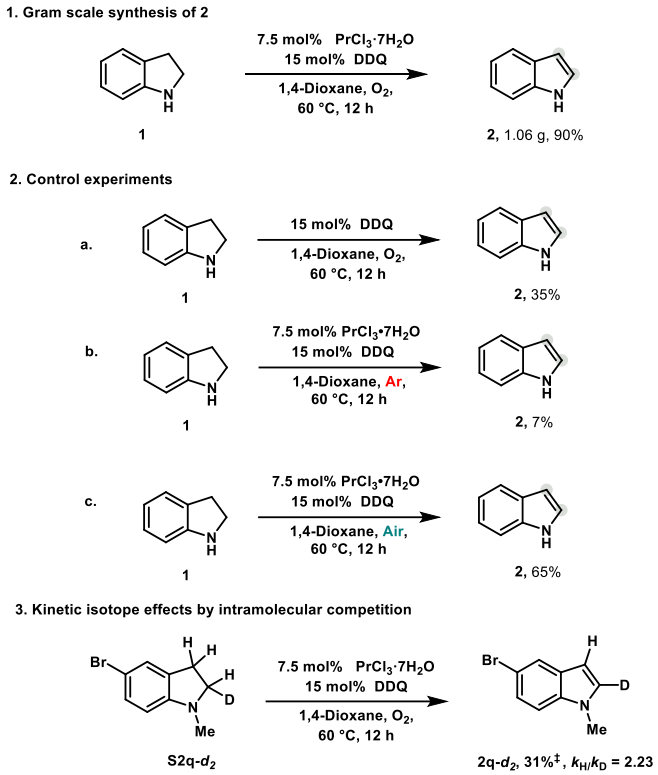

Figure 1. UV-Vis absorption spectra[a].

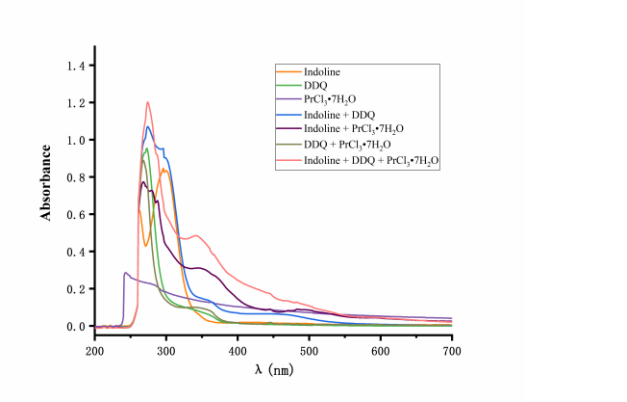

[a]UV-Vis absorption in methyl alcohol (2.5×10^{-4}M) at 22 °C.

In conclusion, we have developed a protocol for rare earth metal-catalyzed aerobic dehydrogenative aromatization to produce a series of unsaturated N-heterocycles. This method demonstrated good substrate compatibility with a wide range of functional groups, including indoline, nifedipine, quinoline, benzoxazole, quinazoline, quinazolone, and β-carboline under mild conditions. Notably, the N1 position of indolines accommodated diverse electron-donating and electron-withdrawing substituents. Our preliminary mechanistic study indicated that the reaction started by the direct coordination of Pr^{3+} with indoline. Further mechanistic investigation and applications of rare earth metal-mediated transformations are ongoing in our lab.

ASSOCIATED CONTENT

Supporting Information

The Supporting Information is available free of chargeat. Experimental procedures, characterizations and analytical data of now compounds; and spectra of NMR (PDF)

AUTHOR INFORMATION

Corresponding Author

Zhenhua Jia - Institute of Advanced Synthesis, School of Chemistry and Molecular Engineering, Jiangsu National Synergetic Innovation Center for Advanced Materials, Nanjing Tech University, Nanjing, 211816, China;orcid.org/0000-0002-5154-4839;
Email: iaszhjia@njtech.edu.cn

Teck-Peng Loh - Division of Chemistry and Biological Chemistry, School of Physical and Mathematical Sciences, Nanyang Technological University, Singapore, 637371, Singapore; orcid.org/0000-0002-2936-337X;
Email: teckpeng@ntu.edu.sg

Authors

Ting Zhang - Institute of Advanced Synthesis, School of Chemistry and Molecular Engineering, Jiangsu National Synergetic Innovation Center for Advanced Materials, Nanjing Tech University, Nanjing, 211816, China.

Yongheng Lv - Institute of Advanced Synthesis, School of Chemistry and Molecular Engineering, Jiangsu National Synergetic Innovation Center for Advanced Materials, Nanjing Tech University, Nanjing, 211816, China.

Zhenguo Zhang - Division of Chemistry and Biological Chemistry, School of Physical and Mathematical Sciences, Nanyang Technological University, Singapore, 637371, Singapore.

Notes

The authors declare no competing financial interests.

ACKNOWLEDGMENT

We thank the financial support from the Start-up Grant of Nanjing Tech University (No. 38274017103, 38037037). T.-P. L thank the financial support from Distinguished University Professor grant (Nanyang Technological University), AcRF Tier 1 grants from the Ministry of Education of Singapore (RG 107/19, RG 11/20 and RT 14/20), and the Agency for Science, Technology and Research (A*STAR) under its MTC Individual Research Grants (M21K2c0114).

REFERENCES

(1) Armelao, L.; Quici, S.; Barigelletti, F.; Accorsi, G.; Bottaro, G.; Cavazzini, M.; Tondello, E. Design of luminescent lanthanide complexes: From molecules to highly efficient photo-emitting materials. *Coord. Chem. Rev*. **2010**, *254*, 487-505.

(2) Beeby, A.; Botchway, S. W.; Clarkson, I. M.; Faulkner, S.; Parker, A. W.; Parker, D.; Williams, J. A. G. Luminescence imaging microscopy and lifetime mapping using kinetically stable lanthanide(III) complexes. *J. Photochem. Photobiol. B Biol.* **2000**, *57*, 83-89.

(3) Zhao, Y.; Wang, Y.; Jin, H.; Yin, L.; Wu, X.; Ma, Y.; Townsend, P. D. Thermoluminescence spectra of rare earth doped magnesium orthosilicate. *J. Alloys Compd*. **2019**, *797*, 13381347.

(4) Klink, S. I.; Hebbink, G. A.; Grave, L.; Van Veggel, F. C. J. M.; Reinhoudt, D. N.; Slooff, L. H.; Polman, A.; Hofstraat, J. W. Sensitized near-infrared luminescence from polydentate triphenylene-functionalized Nd^{3+}, Yb^{3+}, and Er^{3+} complexes. *J. Appl. Phys*. **1999**, *86*, 1181-1185.

(5) (a) Bakker, B. H.; Goes, M.; Hoebe, N.; van Ramesdonk, H. J.; Verhoeven, J. W.; Werts, M. H. V.; Hofstraat, J. W. Luminescent materials and devices: lanthanide azatriphenylene complexes and electroluminescent charge transfer systems. *Coord. Chem. Rev.* **2000**, *208*, 3-16. (b) Malandrino, G.; Fragalà, I. L. Lanthanide "second-generation" precursors for MOCVD applications: Effects of the metal ionic radius and polyether length on coordination spheres and mass-transport properties. *Coord. Chem. Rev.* **2006**, *250*, 1605-1620. (c) Sun, Y.; Wang, Z.; Wu, S.; Zhang, Y.; Shi, F., Lewis acid-catalyzed [4+2] cycloaddition of 3-alkyl-2-vinylindoles with β,γ-unsaturated α-ketoesters. *Green Synth. Catal.* **2022**, *3*, 84-88

(6) (a) Nie, K.; Han, Y.; Wang, C.; Cheng, X. Rare-earth metal-catalyzed hydroboration of unsaturated compounds. *Appl. Organomet. Chem.* **2021**, *36*.1-12. (b) Bousrez, G.; Jaroschik, F. Organic Synthesis with Elemental Lanthanides-Going Beyond Samarium and Ytterbium. *Eur. J. Org. Chem.* **2022**, *e202200202*, 1-16. (c) Prieto, A.; Jaroschik, F. Recent Applications of Rare Earth Complexes in Photoredox Catalysis for Organic Synthesis. *Curr. Org. Chem*. **2022**, *26*, 6-41.

(7) (a) Karnatak, R. C. Rare earth valence in ROx (R = Ce, Pr, Tb; $1.5 \leqslant x \leqslant 2$) studied by X-ray absorption spectroscopy. *J. Alloys Compd.* **1993**, *192*, 64-68. (b) Friedrich, J.; Schneider, D.; Bock, L.; Maichle-Mossmer, C.; Anwander, R. Cerium(IV) Neopentoxide Complexes. *Inorg. Chem.* **2017**, *56*, 8114-8127. (c) Willauer, A. R.; Palumbo, C. T.; Fadaei-Tirani, F.; Zivkovic, I.; Douair, I.; Maron, L.; Mazzanti, M. Accessing the +IV Oxidation State in Molecular Complexes of Praseodymium. *J. Am. Chem. Soc.* **2020**, *142*, 5538-5542. (d) Monteiro, B.; Bandeira, N. A. G.; Lourenco, C.; Lucena, A. F.; Carretas, J. M.; Gibson, J. K.; Marcalo, J. Chemical evidence of the stability of praseodymium(v) in gas-phase oxide nitrate complexes. *Chem.Commun.* **2019**, *55*, 14139-14142. (e) Yin, T.Q.; Liang, Y.; Qu, J. M.; Li, P.; An, R.F.; Xue, Y.; Zhang, M.L.; Han, W.; Wang, G.L.; Yan, Y.D. Thermodynamic and Electrochemical Properties of Praseodymium and the Formation of Ni-PrIntermetallics in LiCl-KCl Melts. *J. Electrochem. Soc.* **2017**, *164*, 835-842. (f) Schumann, H.; Mueller, J.; Bruncks, N.; Lauke, H.; Pickardt, J.; Schwarz, H.; Eckart, K. Organometallic compounds of the lanthanides Tris[(tetramethylethylenediamine)lithium] hexamethyl derivatives of the rare earths. *Organometallics*. **1984**, *3*, 69-74.

(8) Imamoto, T.; Kusumoto, T.; Tawarayama, Y; Sugiura, Y.; Mita, T.; Hatanaka, Y.; Yokoyama, M. Carbon-carbon bond-forming reactions using cerium metal ororganocerium (III) reagents. *J. Org. Chem.* **1984**, *49*, 3904-3912.

(9) Drapo, J. R.; Priefer, R. Praseodymium-Induced Pinacol Formation. *Synth. Commun.* **2008**, *39*, 85-92.

(10) Wu, S.; Li, Y.; Zhang, S. *α*-RegioselectiveBarbier Reaction of Carbonyl Compounds and Allyl Halides Mediated by Praseodymium. *J. Org.Chem.* **2016**, *81*, 8070-8076.

(11) Li, J. L.; Hu, D. C.; Liang, X. P.; Wang, Y. C.; Wang, H. S.; Pan, Y. M. Praseodymium(III)-Catalyzed Regioselective Synthesis of C_3-N-Substituted Coumarins with Coumarins and Azides. *J. Org.Chem.* **2017**, *82*, 9006-9011.

(12) (a) Thansandote, P.; Lautens, M. Construction of nitrogen-containing heterocycles by C-H bond functionalization. *Chem. Eur. J.* **2009**, *15*, 5874-83. (b) Kaur, N. Multiple nitrogen-containing heterocycles: Metal and non-metal assisted synthesis. *Synth. Commun.* **2018**, *49*, 1633-1658. (c) Silva, T. S.; Rodrigues, M. T.; Santos, H.; Zeoly, L. A.; Almeida, W. P.; Barcelos, R. C.; Gomes, R. C.; Fernandes, F. S.; Coelho, F. Recent advances in indoline synthesis. *Tetrahedron.* **2019**, *75*, 2063-2097. (d) Bera, A.; Bera, S.; Banerjee, D. Recent advances in the synthesis of N-heteroarenes via catalytic dehydrogenation of N-heterocycles. *Chem. Commun*. **2021**, *57*, 13042-13058. (e) Kumar, P.; Nagtilak, P. J.; Kapur, M. Transition metal-catalyzed C–H functionalizations of indoles. *New J. Chem.* **2021**, *45*, 13692-13746.

(13) (a) Yin, P.; Loh, T.-P. Intermolecular Hydroamination between Nonactivated Alkenes and Aniline Catalyzed by Lanthanide Salts in Ionic Solvents. *Org. Lett*. **2009**, *11*, 3791-3793. (b) Dong, S.; Chen, J.; Qiao, K.; Fang, J.; Yang, Y.; Maron, L.; Liu, B. Insights into Rare-Earth Metal Complex-Mediated Hydroamination. *ACS Catal.* **2021**, *11*, 3790-3800. (c) Wartenberg, N.; Raccurt, O.; Bourgeat-Lami, E.; Imbert, D.; Mazzanti, M. Multicolour optical coding from a series of luminescent lanthanide complexes with a unique antenna. *Chem. Eur. J*. **2013**, *19*, 3477-3482.

(14) (a) Jiang, X.; Tang, W.; Xue, D.; Xiao, J.; Wang, C. Divergent Dehydrogenative Coupling of Indolines with Alcohols. *ACS Catal.* **2017**, *7*, 1831-1835. (b) Zhou, C. Z.; Zhao, Y. R.; Tan, F. F.; Guo, Y. J.; Li, Y. Utilization of renewable formic acid from lignocellulosic biomass for the selective hydrogenation and/or N-methylation. *ChemCatChem.* **2021**, *13*, 4724-4728. (c) Li, B.; Wendlandt, A. E.; Stahl, S. S. Replacement of Stoichiometric DDQ with a Low Potential *o*-Quinone Catalyst Enabling Aerobic Dehydrogenation of Tertiary Indolines in Pharmaceutical Intermediates. *Org. Lett*. **2019**, *21*, 1176-1181. (d) Yoo, H. S.; Yang, Y. S.; Kim, S. L.; Son, S. H.; Jang, Y. H.; Shin, J. W.; Kim, N. J. Syntheses of 1*H*-Indoles, Quinolines, and 6-Membered Aromatic N-Heterocycle-Fused Scaffolds via Palladium(II)-Catalyzed Aerobic Dehydrogenation under Alkoxide-Free Conditions.*Chem Asian J*. **2021**, *16*, 3469-3475.

(15) Zhang, D.; Iwai, T.; Sawamura, M. Ir-Catalyzed Reversible AcceptorlessDehydrogenation/Hydrogenation of N-Substituted and Unsubstituted Heterocycles Enabled by a Polymer-Cross-Linking Bisphosphine. *Org. Lett.* **2020**, *22*, 5240-5245.

(16) Chen, W.; Tang, H.; Wang, W.; Fu, Q.; Luo, J. Catalytic Aerobic Dehydrogenatin of N-Heterocycles by N-Hydoxyphthalimide. *Adv. Synth. Catal.* **2020**, *362*, 3905-3911.

(17) Youn, S. W.; Ko, T. Y. Metal-Catalyzed Synthesis of Substituted Indoles. *Asian J. Org. Chem.* **2018**, *7*, 1467-1487.

(18) Kumar, P.; Nagtilak, P. J.; Kapur, M. Transition metal-catalyzed C–H functionalizations of indoles. *New J. Chem*. **2021**, *45*, 13692-13746.

(19) Das, S.; Mondal, R.; Chakraborty, G.; Guin, A. K.; Das, A.; Paul, N. D. Zinc Stabilized Azo-anion Radical in Dehydrogenative Synthesis of N-Heterocycles. An Exclusively Ligand Centered Redox Controlled Approach. *ACS Catal.* **2021**, *11*, 7498-7512.

(20) Niu, X.; Yang, L. Manganese(III) Acetate Catalyzed Aerobic Dehydrogenation of Tertiary Indolines, Tetrahydroquinolines and an N-Unsubstituted Indoline. *Adv. Synth. Catal.* **2021**, *363*, 4209-4215.

(21) Luo, J.; Chen, W.; Zhang, B.; Tang, H. A Mild and Efficient Catalytic Aerobic Oxidative Dehydrogenation of N-Pyridylindolines. *Chin. J. Org. Chem*. **2021**, *41*, 8-12.

(22) (a) Jiang, P.; Chen, S.; Huang, H.; Hu, K.; Xia, Y.; Deng, G.-J., Metal-free synthesis of indolo [2,3-b] indoles through aerobic cascade dehydrogenative aromatization/oxidative annulation. *Green Synth. Catal.* **2021**, *2*, 78-81. (b) Rago, A. J.; Dong, G., Synthesis of indoles, indolines, and carbazoles via palladium-catalyzedC–H activation. *Green Synth. Catal.* **2021**, *2*, 216-227. (c) Su, B.; Xu, L.; Xu, X.; Wang, L.; Li, A.; Lin, J.; Ye, L.; Yu, H., Redesign of a short-chaindehydrogenase/reductase for asymmetric synthesis of ethyl (R)-2-hydroxy-4-phenylbutanoatebased on perresidue free energy decomposition and sequence conservatism analysis. *Green Synth. Catal.* **2020,** *1*, 150-159.